

IMPLEMENTATION OF A BIO-INSPIRED TWO-MODE STRUCTURAL HEALTH MONITORING SYSTEM

Tzu-Kang Lin¹, Li-Chen Yu², Chang-Hung Ku³,
Kuo-Chun Chang⁴, Anne Kiremidjian⁵

¹Research Fellow, National Center for Research on Earthquake Engineering,
tklin@ncree.org

²³Graduate Student, Department of Civil Engineering, National Taiwan University,
b95501011@ntu.edu.tw, b95501031@ntu.edu.tw

⁴Professor, Department of Civil Engineering, National Taiwan University,
ciekuo@ccms.ntu.edu.tw

⁵Professor, Department of Civil and Environmental Engineering, Stanford
University, ask@stanford.edu

Keywords: Structural Health Monitoring, Naïve Bayes, Bio-inspired.

Abstract. A bio-inspired two-mode structural health monitoring (SHM) system based on the Naïve Bayes (NB) classification method is discussed in this paper. For the micro-vibration mode, a two-tier auto-regression with exogenous (AR-ARX) process is used to extract the expression array from the recorded structural time history while an ARX process is applied for the analysis of the earthquake mode. The health condition of the structure is then determined using the NB classification method. To verify the performance and reliability of the SHM algorithm, a downscaled eight-storey steel building was used as the benchmark structure. The structural response from different damage levels and locations was collected and incorporated in the database to aid the structural health monitoring process. Preliminary verification has demonstrated that the structure health condition can be precisely detected by the proposed algorithm. To implement the developed SHM system in a practical application, a SHM prototype was developed, which consists of three separate modules namely, the input sensing module, the transmission module, and the SHM platform. The vibration data is first measured by the deployed sensor, and subsequently the SHM mode corresponding to the desired excitation is chosen automatically to quickly evaluate the health condition of the structure. Test results from the ambient vibration and shaking table test showed that the condition and location of the benchmark structure damage can be successfully detected by the proposed SHM prototype system, and the information is instantaneously transmitted to a remote server to facilitate real-time monitoring. Implementing the bio-inspired two-mode SHM practically has been successfully demonstrated.

1 INTRODUCTION

Recently, an increasing number of infrastructures and buildings all over the world have been unexpectedly damaged or have collapsed due to aging and long-term material degradation. Even though most of these structures have been periodically examined or monitored using modern techniques, these catastrophic failures continue to happen. Due to the existence of a large number of aging buildings, structural health monitoring (SHM) has become an important issue in civil engineering and must go hand in hand with the current research to improve the capacity of structures and to develop a safer design method.

The multidisciplinary research field of SHM was first proposed in the area of aerospace engineering. Accompanied by the development of advanced sensors, SHM was then subsequently developed for applications such as aerospace engineering, mechanical engineering, and civil engineering. However, contrary to the other two fields, civil engineering has faced specific challenges with respect to SHM development. For example, large-scale monitoring applications in civil engineering often using customized monitoring equipment make monitoring a difficult task. Unlike the mass production frequently seen in the field of mechanical engineering where a specific SHM module can be applied to all products to save time and cost, SHM devices used in a structure are commonly customized to cater to the demand and functionality of that particular structure. In addition, the unique requirements of the exterior of structural elements such as fire proofing or indoor appearance requirements, hinder the installation of a SHM system.

The first SHM systems consisted of simple instrumentation. With development in sensor and signal processor technology, SHM systems based on these techniques were capable of detecting the structural health of aircrafts and with the help of a preventive maintenance system greatly extended the lifetime of aircrafts [Hickman et al. 1991]. In 1998, a coordination was achieved between universities, government agencies, and industry, and an innovative SHM assessment method for the overall structural condition of structures was proposed by incorporating the basic concept of system identification [Aktan et al. 1998].

To reduce both the high cost and time required for the on-site cable installation of a traditional SHM system, wireless technology was introduced in the field of SHM. For example, a new method combining the advantages of an advanced sensor and the wireless technique was proposed by Pines et al., to remotely monitor the condition of various infrastructures in 1998. Data collected by the sensors from a structure can be remotely and wirelessly transmitted back to the server and processed by the SHM system on a computer giving an indication of both the damage location and the level of damage [Pines et al. 1998]. Other SHM systems integrating sensors, micro processors, and a wireless transmitter have also been developed, and targets like high speed, accuracy, and low-cost are gradually being accomplished [Tanner 2003, Wang et al. 2007].

In subsequent years, a tiny laser scanner has been developed which can be installed in different locations of the structure for scanning cracks and monitoring fatigue. Based on its specific characteristics, the device can be incorporated in aircrafts, railways, and civil structures [Buckner et al. 2008]. Due to extensive research and subsequent achievements over the past decade, the original SHM concept for structures is being used extensively today to monitor specific structure characteristics under both ambient and forced vibrations. A study conducted by Zimmerman et al. has also proved that data can be collected reliably and processed by a pure wireless

SHM system [Zimmerman et al. 2008]. A SHM system based on a hybrid wireless network has also been verified for its feasibility in the laboratory, and several structural response parameters have been effectively monitored on site for a rapid assessment of the conditions [Mascarenas et al. 2010].

In addition to the development of the SHM system, algorithms focusing on certain specific applications have also been proposed. Contrary to the original concept wherein sensors were installed on the structure to identify the location of the damage, researchers have started to employ customized SHM software to enable a more accurate diagnosis. SHM software development was initiated in the field of aerospace engineering in the year 2000 to reduce the heavy operating and maintenance fees and to further extend the aircraft lifetime [Boller 2000]. Around the same time, various SHM algorithms for infrastructures were developed in the field of civil engineering to offer more precise detection results using certain physical SHM techniques. For example, Johnson et al. utilized local vibration signals in combination with an intelligent diagnosis algorithm to demonstrate the feasibility of a distributed SHM system for damage location and monitoring [Johnson et al. 2004]. Another algorithm based on wavelet analysis to detect the location and the level of damage for the four-story benchmark structure proposed by the American Society of Civil Engineers (ASCE) was also developed. The efficacy of this SHM system was demonstrated by drawing a comparison with an established finite element model for wind loading [Hera and Hou 2004].

Studies on the selection of proper structural parameters for the SHM have been widely conducted over the past decade. Unlike the traditional identification method, parameters selected by the genetic algorithm (GA) have shown certain unique advantages of the SHM [Udwadia and Proskurowski 1998]. The monitoring of large-scale structures is a constant challenge faced by engineers especially when the measured data contains high-frequency noise. Thus, to overcome the above problems, a new statistical SHM system based on the Support Vector Machine (SVM) was proposed. This system was found to be highly reliable under different types and different levels of noise intensity [Zhang et al. 2006]. Furthermore, a new method integrating the Autoregressive Moving Average (ARMA) models and statistical theory was used to analyze the structural response in the time domain [Carden and Brownjohn 2008]. However, as mentioned above, researchers are still faced with the problem of selecting the proper parameters for the SHM algorithm.

As the bio-inspired concept was introduced in the field of engineering, researchers began to seek for possible solution inspired from the nature. The concept of gene expression monitoring was first proposed and implemented by Golub [Golub et al. 1999]. This method offered a new way to classify cancer cells and gave rise to further research in detecting diseases from a gene expression array. The results from the research ignited a new research field, and subsequent research by Slonim et al. also demonstrated the feasibility of combining the NB algorithm and the DNA array data for multi-class cancer diagnosis [Slonim et al. 2000]. In order to obtain high accuracy and overcome obstacles such as high manpower and high equipment costs for monitoring structures, a new two-mode SHM system based on bioinformatics has been proposed in this paper. The proposed system is composed of two main parts: the SHM software and SHM hardware. The basic theory of the SHM algorithm has been described in section 2. The preliminary verification of the proposed system has then been carried out on an eight-storey downscaled benchmark at NCREE in section 3. The proposed SHM system has then been implemented on a mobile SHM prototype in

section 4. Section 5 discusses the practical verification of the integrated SHM system, and based on the results, a summary and conclusion have been included.

2 THE PROPOSED SHM ALGORITHM

As the bio-inspired concept for engineering is a broadly discussed topic, a novel SHM algorithm employing array expression data as the Deoxyribonucleic acid (DNA) of the structures is proposed in this research. Based on the type of vibration which can either be strong ground excitation or ambient vibration, the recorded time history is converted using an auto-regression-auto-regression with exogenous (AR-ARX) process for micro-vibration and an ARX process for earthquake excitation. The AR regression model has proven to be effective in the illustration of the structure model under pure ambient vibration while the ARX model is suitable for significant external excitation conditions [Ljung, 1986]. A series of research conducted by Sohn et al. has also demonstrated the advantage of using the chosen AR-ARX model for unknown excitation between pure ambient and strong ground excitation [Sohn et al. 2000][Sohn and Farrar, 2001]. The obtained array is then compared using the Naïve Bayes (NB) classification method which is the core of the SHM algorithm to detect the damage condition and location as shown in Figure 1. The basic description of each part is briefly summarized as follows:

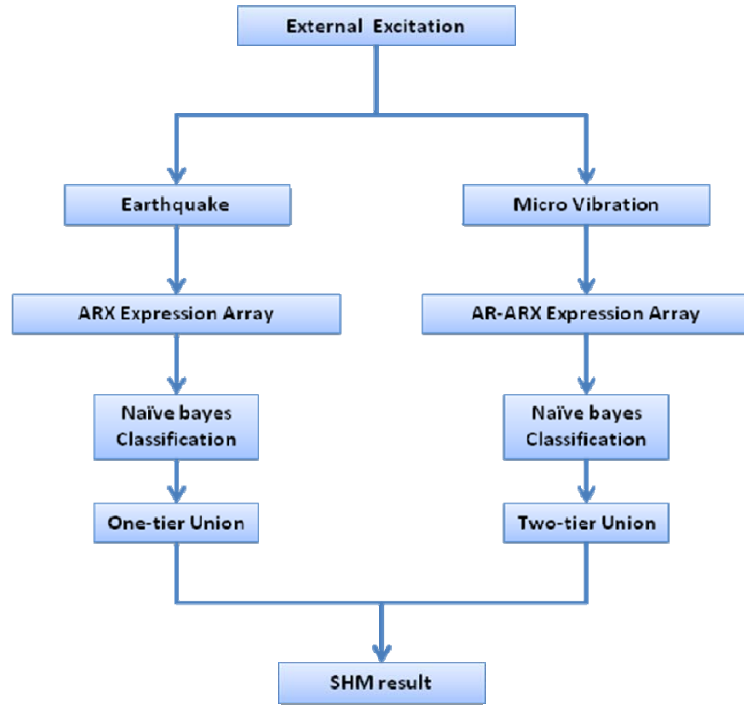


Figure 1: Flowchart of the SHM Algorithm

2.1 THE ARX EXPRESSION ARRAY

The array expression data for earthquake excitation is first extracted using the established ARX model. The measured acceleration response is used in the regression model to precisely describe the behavior of the structure.

For a single-input-single-output (SISO) system, the relationship between the input and output can be expressed as a linear differential equation, given by:

$$y(t) + a_1 y(t-1) + \dots + a_{n_a} y(t-n_a) = b_1 u(t-1) + \dots + b_{n_b} u(t-n_b) + e(t) \quad (1)$$

Where n_a and n_b represent the output and input steps used for regression, respectively.

As $e(t)$ is commonly treated as a random white-noise error in the differential equation, the model is termed the equation error model, and the adjustable parameters can be shown as:

$$\theta = [a_1 \ a_2 \ \cdots \ a_{n_a} \ b_1 \ \cdots \ b_{n_b}]^T \quad (2)$$

By assuming

$$A(q) = 1 + a_1 q^{-1} + \cdots + a_{n_a} q^{-n_a} \quad (3)$$

$$B(q) = b_1 q^{-1} + \cdots + b_{n_b} q^{-n_b} \quad (4)$$

The equation can be rewritten as:

$$A(q)y(t) = B(q)u(t) + e(t) \quad (5)$$

The regression model described in equation 5 is a typical example of the ARX model shown in Figure 2 where the AR part is denoted by $A(q)y(t)$, and X is the external input expressed as $B(q)u(t)$. The model becomes a typical AR model if the external excitation X is excluded as depicted in Figure 3, and will be used as a part of the AR-ARX model later on.

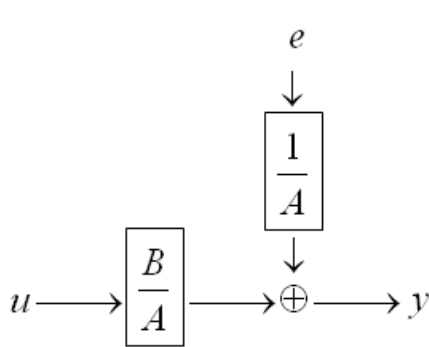


Figure 2: The ARX Model

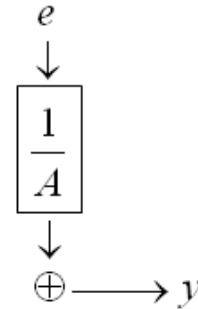


Figure 3: The AR Model

2.2 THE AR-ARX EXPRESSION ARRAY

The array expression data for the micro-vibration mode of the two-mode SHM system is extracted using the two-tier AR-ARX model. As the velocity response of the structure is more sensitive compared to the acceleration under conditions of micro-vibration, it is employed in the regression model. The AR-ARX model is explained briefly below.

The velocity response $x(t)$ is first input to an AR regression model with p terms

$$x(t) = \sum_{j=1}^p \phi_{xj} x(t-j) + e_x(t) \quad (6)$$

Where $e_x(t)$ is the white-noise input signal defined as the external excitation of the AR model.

By assuming that the error generated from the model depicted in Figure 2 is the input of equation 7, the model combining these two parts represents the proposed AR-ARX model illustrated in Figure 4. The corresponding equation can be expressed as

$$x(t) = \sum_{i=1}^{n_a} a_i x(t-i) + \sum_{j=1}^{n_b} b_j e_x(t-j) + \varepsilon_x(t) \quad (7)$$

Where $e_x(t)$ is the error generated by the first AR model; n_a and n_b are the order for the input and output, respectively. The coefficients calculated from the AR-ARX model are then used in the micro-vibration mode of the SHM system.

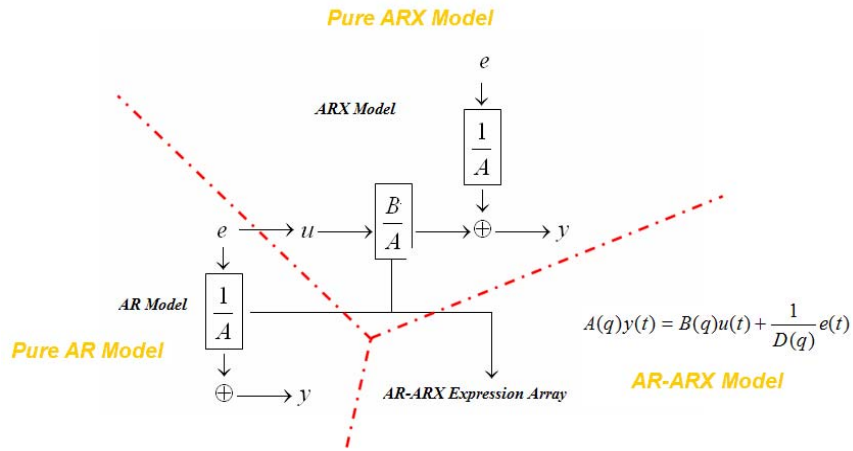


Figure 4: The AR-ARX Model

2.3 THE NAÏVE BAYES (NB) ALGORITHM

The NB algorithm which forms the core of the SHM software is a classification method established on the basics of probability theory. The a posteriori probability is estimated from the prior probability and can be expressed as a conditional probability. The test sample is inputted to the NB algorithm with a Bayes probability distribution defined by two parameters, namely, the mean value and standard deviation to determine the final probability.

The proposed methodology attempts to investigate every coefficient as the DNA of the monitoring structure as opposed to the traditional SHM method, where the health condition is usually determined by only comparing the prediction error of each pre-established regression model. The probability of a specific coefficient of the array expression data is calculated based on the presumed Gaussian distribution for an individual coefficient, which was proven to be easily satisfied. The final damage type is then determined by combining the total probability of the array expression data with the maximum a posteriori probability.

The NB algorithm can be simplified as:

$$Class(x) = \arg \max_i \left\{ \sum_{\text{coefficient}} \left[\log(\sigma_i^g) + 0.5 \left(\frac{x^g - \mu_i^g}{\sigma_i^g} \right)^2 \right] \right\} \quad (8)$$

Where i is the array number of the test sample; μ_i^g is the mean value of class i and g th coefficient; σ_i^g is the standard deviation of class i and g th coefficient, and x_i^g is the g th coefficient value of the test sample.

3 PRELIMINARY VERIFICATION

To verify the feasibility of the proposed SHM system in a practical structure, a series of experiments were conducted on the eight-storey downscale specimen at the National Center for Research on Earthquake Engineering (NCREE). As shown in Figure 5, eight high-sensitivity velocity meters and eight accelerometers were deployed on the specimen to measure the floor response under micro and earthquake vibration conditions, with the sampling rate set at 200 Hz.

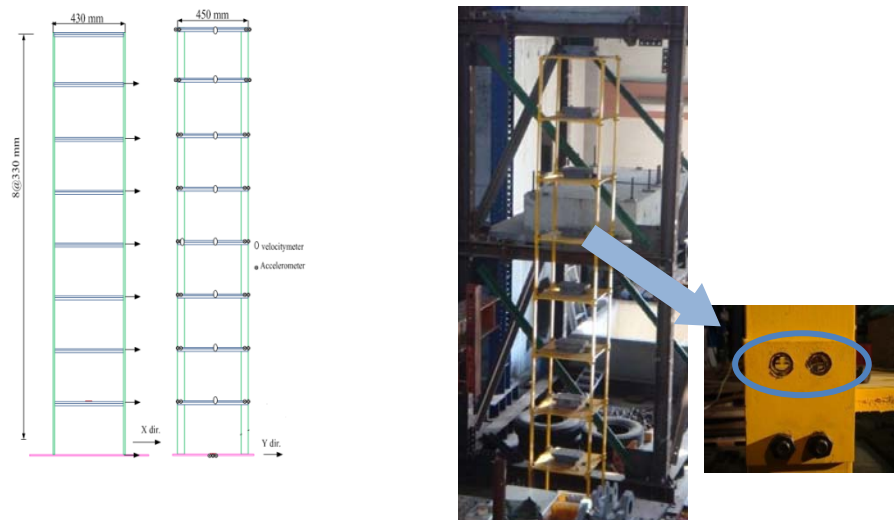


Figure 5: the eight-story SHM Benchmark at NCREE

Signals measured from the ambient vibration in the daily life are first used by the proposed system to enhance its practicability. The structural damages were classified into five major groups for 19 different damage conditions and were simulated by loosening four of the 16 bolts in each floor (1/4 of the beam-column connections). The dataset for the experiment was collected at night to avoid or substantially suppress the unwanted noise arising from machine operation or human activity in the laboratory which aimed to improve the reliability of the structural feature arrays. The 19 damage conditions are listed in Table 1, and 90 time histories each subjected to every damage condition for 20 seconds were recorded. The 19 damage conditions were achieved by switching the location of the loosened fasteners.

Concurrently, the structural response of the benchmark under earthquake excitation conditions was recorded by conducting the shaking table test at NCREE to verify the operation of the earthquake mode of the system. A list of the 11 damage conditions achieved by switching the location of the loosened fasteners is listed in Table 2, and 30 time histories including the 1940 El Centro, 1995 Kobe, TCU 072 and TCU 129 station record of the Chi-Chi earthquake were recorded for different peak ground acceleration (PGA) values for every damage condition.

Table 1: Damage Condition for the Micro-vibration Experiment

| Damage Condition Number | Damage Level | Damage Location |
|-------------------------|--------------|-----------------|
| 1 | Undamaged | None |
| 2 | Slight | 1F |
| 3 | | 2F |
| 4 | | 3F |
| 5 | | 4F |
| 6 | | 5F |
| 7 | | 6F |
| 8 | | 7F |
| 9 | | 8F |
| 10 | Moderate | 1 & 2F |
| 11 | | 3 & 4F |
| 12 | | 5 & 6F |
| 13 | | 7 & 8F |
| 14 | Severe | 1 & 2 & 3F |
| 15 | | 4 & 5 & 6F |
| 16 | | 6 & 7 & 8F |
| 17 | Extreme | 1 & 2 & 3 & 4F |
| 18 | | 5 & 6 & 7 & 8F |
| 19 | Ultimate | 1-8F |

Table 2: Damage Condition for the Earthquake Excitation Experiment

| Damage Condition Number | Damage Level | Damage Location |
|-------------------------|--------------|-----------------|
| 1 | Undamaged | None |
| 2 | Slight | 1F |
| 3 | | 2F |
| 4 | | 3F |
| 5 | | 5F |
| 6 | | 7F |
| 7 | | Moderate |
| 8 | 5 & 6F | |
| 9 | Severe | 1 & 2 & 3F |
| 10 | | 4 & 5 & 6F |
| 11 | Ultimate | 1 & 2 & 3 & 4F |

The micro-vibration mode of the SHM algorithm was first verified. Three fundamental parameters (p , a , and b) of the basic AR-ARX model described in equations 6 and 7, were designed to be 10-8-4 based on the rule of thumb for system identification proposed by Ljung [Ljung, 1986]. The ratio of the coefficients a and b is set to 2, and the optimal value of p is then determined. Ljung suggests that better identification results can be obtained when the sum of a and b is smaller than p . However, better structural behavior can be achieved by adjusting the value of p from 12 to 10 using an optimization process.

The advantage of utilizing array expression data for SHM was also evaluated using three different array orders, namely, 30-24-12, 40-32-16, and 50-40-20 based on the format specified above to decipher the optimal array for the system while no significant difference of computation overhead was observed. To enable independent testing of the SHM system, 10 patterns selected from the database were used to verify the system performance. Figure 6 depicts the results of all 19 damage conditions which were obtained from the velocity meter located on the sixth floor (V6). The AR-ARX order increased from 30-24-12 in the top subplot to the final 50-40-20 in the bottom subplot. The 19 damage conditions are indicated in the longitudinal axis as UN, S1, S2, S3, S4, S5, S6, S7, S8, M12, M34, M56, M78, S123, S456, S678, E1234, E5678, and U12345678, where UN represents undamaged; S represents slight damage; M represents moderate damage; S indicates severe damage; E indicates extreme damage and U indicates ultimate damage. The detected damage condition is reflected in the latitudinal bar. The individual bars for each damage condition express all ten testing patterns. The numbers in the longitudinal axis represents the 19 damage conditions, and the diagnosis result is indicated in the latitudinal axis which should correspond to the same value in the X-axis. As demonstrated in Figure 6, the classification success rate can reach 100% by the proposed system for the 50-40-20 form which can be chosen as the optimal array for micro-vibration except damage conditions 3, 6, and 8 where the success rates are 80%, 90%, and 80%, respectively.

The optimal ARX configuration for earthquake excitation conditions was determined using the collected database. Similarly, the two fundamental parameters (a and b) of the basic ARX model described earlier were designed to have a form 8-4. The advantage of utilizing array expression data for SHM was again evaluated using three different array orders, namely, 48-24, 56-28, and 64-32 based on the 8-4 form. Five patterns recorded from the established database were used to verify the system performance. The ARX order was increased from 48-24 in the top subplot, to the final 64-32 form in the bottom subplot. The individual bars, as show in Figure 7, expressed all five testing patterns. The 11 damage conditions are included in the longitudinal axis as UN, S1, S2, S3, S5, S7, M12, M56, S123, S456, and U1234, where UN represents undamaged; S represents slight damage; M indicates moderate damage; S indicates severe damage, and U indicates ultimate damage. Similarly, the latitudinal bar reflects the detected damage condition while the actual damage condition is marked along the longitudinal axis. Structural damage was again correctly predicted by the system for the 64-32 form. The success rates are approximately 60% for damage conditions 8 and 9 and 80% for damage conditions 1, 2, 3, 4, and 7. This array was then chosen to represent the optimal array for earthquake excitation.

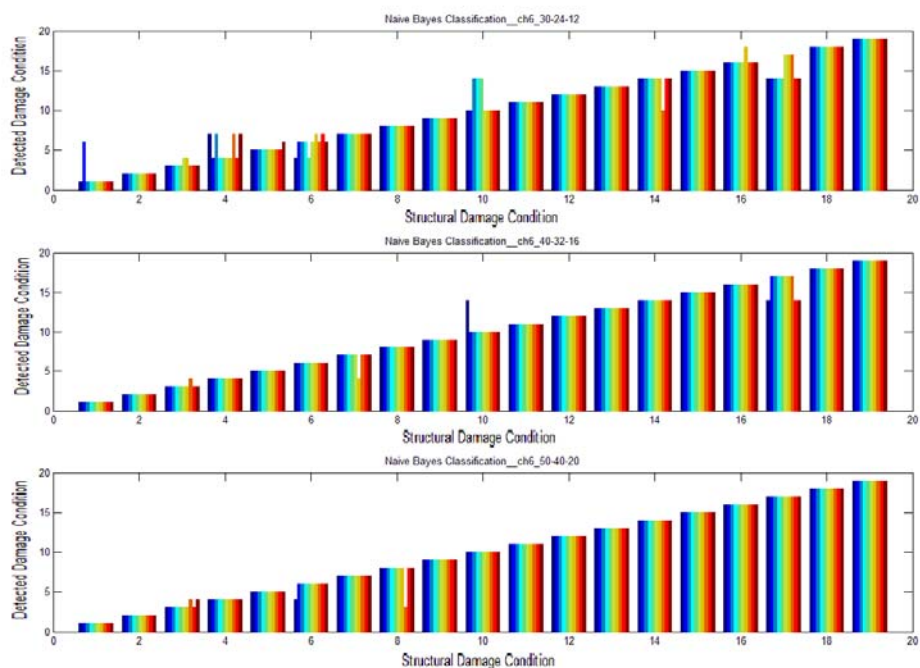


Figure 6: Verification under Micro Vibration

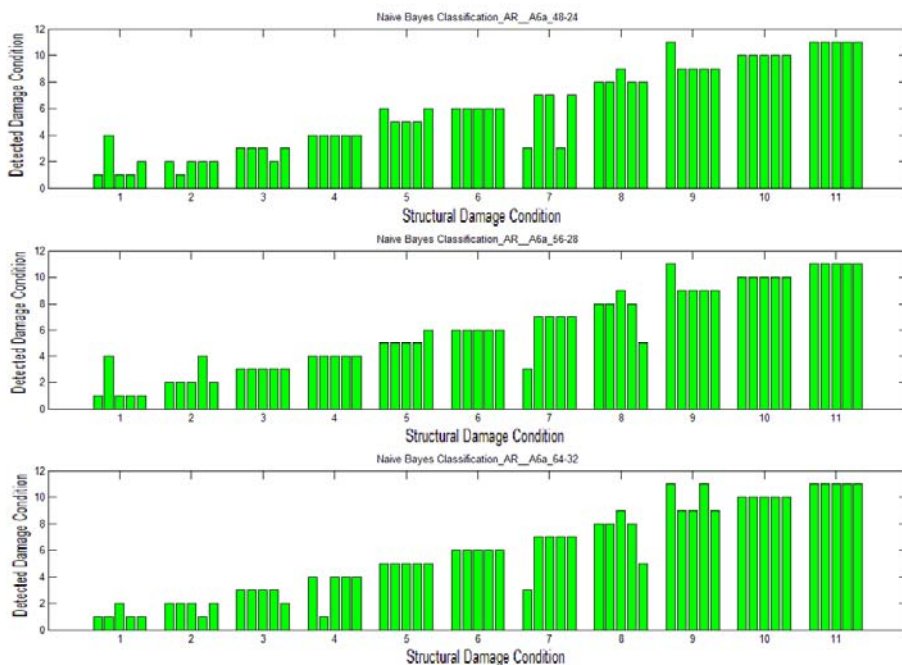


Figure 7: Verification under Earthquake Excitation

The union concept of multi-events or sensors has been introduced to achieve further improvement in the accuracy and reliability of the SHM system. The final SHM result can be determined by choosing the condition with the highest accumulated probability. Since earthquake excitations are infrequent in occurrence, only the union concept with three sensors was applied for earthquake excitation. Simultaneously, the micro-vibration mode was tested using three sensors on their respective floors (6F, 7F, and 8F) in the first union, and the results of these three different events were then combined to obtain a more accurate result. The verification of the two-mode system is summarized as follows: Table 3 shows the results obtained for earthquake excitation, and Table 4 depicts the outcome of the micro-vibration tests.

As shown in Table 3, the diagnosis result for three separate classes of earthquakes indicates almost the same damage condition and only a slight variation was observed for damage conditions 1, 3, 8, and 9. However, the approximate damage condition and location can still be rapidly and correctly determined after the occurrence of an earthquake. In addition, a more precise result can be achieved especially in the micro-vibration detection mode. Only a slight error was observed following the application of the first union of the three sensors, and the second-layer union guaranteed a reliable result. In short, the reliability of the two-mode SHM system has been demonstrated by the preliminary verification tests, indicating that the health condition of the structure under both earthquake excitation and micro-vibration conditions can be accurately detected by the proposed system.

Table 3: SHM result with the Union Concept under Earthquake Excitation Mode

| Damage Condition Number | Event 1 | Event 2 | Event 3 |
|-------------------------|---------|---------|---------|
| 1 | 1 | 1 | 2 |
| 2 | 2 | 2 | 2 |
| 3 | 3 | 2 | 3 |
| 4 | 4 | 4 | 4 |
| 5 | 5 | 5 | 5 |
| 6 | 6 | 6 | 6 |
| 7 | 7 | 7 | 7 |
| 8 | 8 | 8 | 9 |
| 9 | 11 | 9 | 9 |
| 10 | 10 | 10 | 10 |
| 11 | 11 | 11 | 11 |

Table 4: SHM result with the Union Concept under Micro-Vibration Mode

| Damage Condition Number | Event 1 | Event 2 | Event 3 | Final result |
|-------------------------|------------------|------------------|------------------|--------------|
| 1 | 1 (1/1/1) | 1 (1/1/1) | 1 (1/1/1) | 1 |
| 2 | 2 (2/2/2) | 2 (2/2/2) | 2 (2/2/2) | 2 |
| 3 | 3 (3/3/3) | 3 (3/3/3) | 3 (3/3/4) | 3 |
| 4 | 4 (4/4/4) | 4 (4/4/4) | 4 (4/4/4) | 4 |
| 5 | 5 (5/5/5) | 5 (5/5/5) | 5 (5/5/5) | 5 |
| 6 | 6 (4/6/6) | 6 (6/4/6) | 6 (6/6/6) | 6 |
| 7 | 7 (7/7/7) | 7 (7/7/7) | 7 (7/7/7) | 7 |
| 8 | 8 (8/8/8) | 8 (8/8/3) | 8 (8/8/8) | 8 |
| 9 | 9 (9/9/9) | 9 (9/9/9) | 9 (9/9/9) | 9 |
| 10 | 10 (10/10/10) | 10 (10/10/10) | 10 (10/10/10) | 10 |
| 11 | 11 (11/11/11) | 11 (11/11/11) | 11 (11/11/11) | 11 |
| 12 | 12 (12/12/12) | 12 (12/12/12) | 12 (12/12/12) | 12 |
| 13 | 13 (13/13/13) | 13 (13/13/13) | 13 (13/13/13) | 13 |
| 14 | 14 (14/14/14) | 14 (14/14/14) | 14 (14/14/14) | 14 |
| 15 | 15 (15/15/15) | 15 (15/15/15) | 15 (15/15/15) | 15 |
| 16 | 16 (16/16/16) | 16 (16/16/16) | 16 (16/16/16) | 16 |
| 17 | 17 (17/17/17) | 17 (17/17/17) | 17 (17/17/17) | 17 |
| 18 | 18 (18/18/18) | 18 (18/18/18) | 18 (18/18/18) | 18 |
| 19 | 19 (19/19/19) | 19 (19/19/19) | 19 (19/19/19) | 19 |

As mentioned above, the performance of the proposed SHM system has been successfully demonstrated in dealing with damage conditions included in the system repository. However, it is impossible to include all possible damage conditions and structure locations into the SHM database. To verify the robustness of the proposed SHM algorithm, the system was examined by utilizing several damage conditions excluded from the original database. It is expected that the approximate damage condition and location can be detected.

Three damage conditions from both the micro-vibration and earthquake excitation modes were considered, and the rest damage conditions in Tables 1 and 2 were renumbered. For the micro-vibration mode, conditions selected included slight damage on the 5th floor, moderate damage on the 3rd and 4th floors, and severe damage on the 4th& 5th& 6th floors. For the earthquake excitation mode, slight damage on the 7th floor, moderate damage on the 5th and 6th floors, and severe damage on the 4th, 5th, and 6th floors were chosen as the test conditions. The array expression data was input to the SHM algorithm to determine the corresponding damage condition. As shown in Figure 8, the detected damage conditions are indicated by conditions 5, 9 and 12 which reflect the damage condition closest to the actual damage condition with an accuracy of 100%, 70%, and 60%, respectively. Meanwhile, the damage conditions for the earthquake excitation mode shown in Figure 9 were found to be condition 5, 6, and 7 with an accuracy of 80%, 70%, and 70%, respectively. These results strongly support the reliability of the proposed SHM algorithm for use in practical applications wherein the most likely damage condition can be approximated by utilizing the inherent interpolation or extrapolation capability.

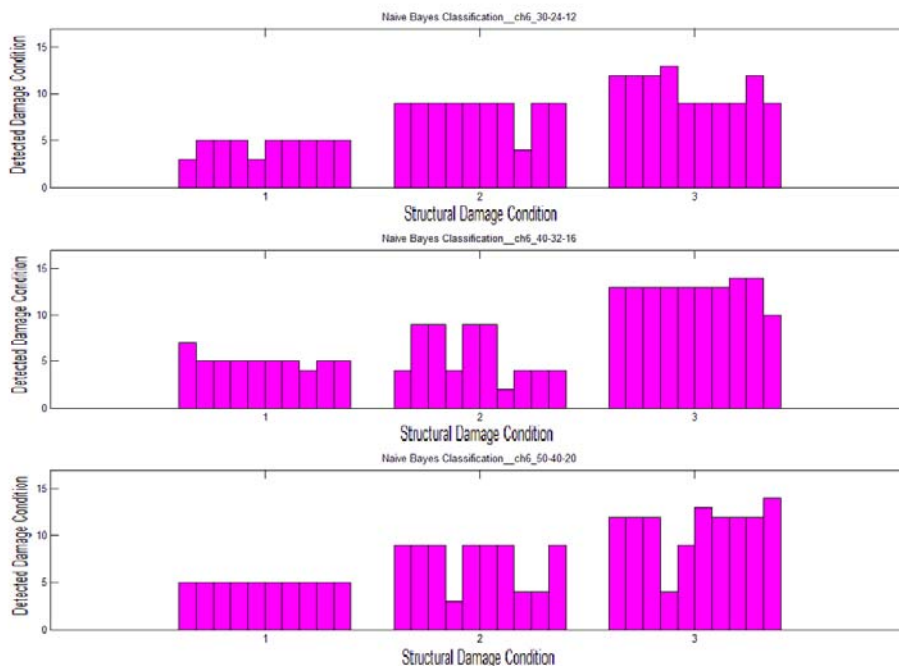


Figure 8: Verification of Unknown Damage Condition under Micro Vibration

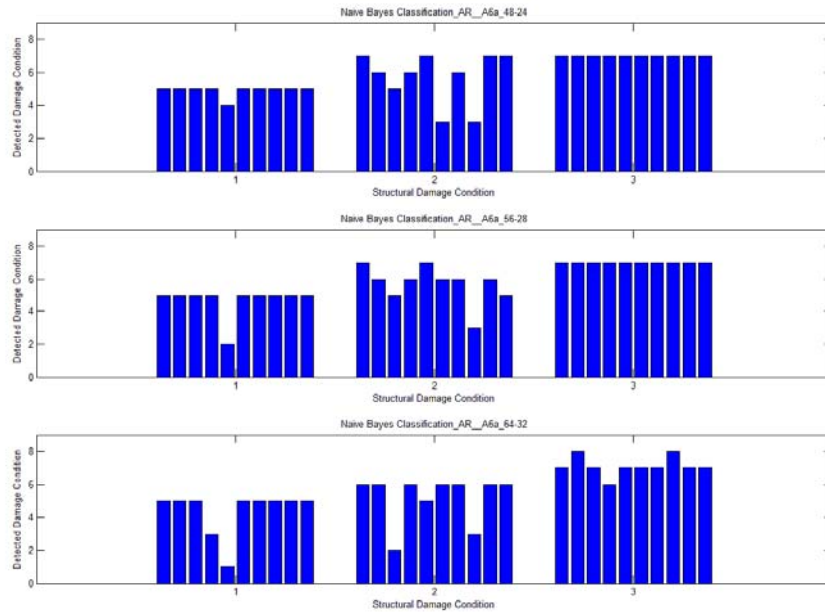


Figure 9: Verification of Unknown Damage Condition under Earthquake Excitation

4 MOBILE SHM PROTOTYPE

In order to implement the bio-inspired SHM system practically, a mobile SHM prototype was developed. As shown in Figure 10, the SHM prototype is composed of three fundamental parts including the sensing input module, the SHM platform for instrumentation and data processing, and the general packet radio service (GPRS) transmission module for conveying the final results to the remote server. To further enhance the mobility of the SHM prototype, a customized silver module depicted in Figure 10 is used for voltage stabilization and power regulation of the sensing unit and data processing center. The vibration data is first measured by the deployed sensor and is subsequently transmitted through the input module to the built-in microprocessor. The acceleration and velocity of the structure are both measured simultaneously to evaluate its structural health condition. In addition, by connecting multiple SHM prototypes, the system can be extended to form a SHM network.

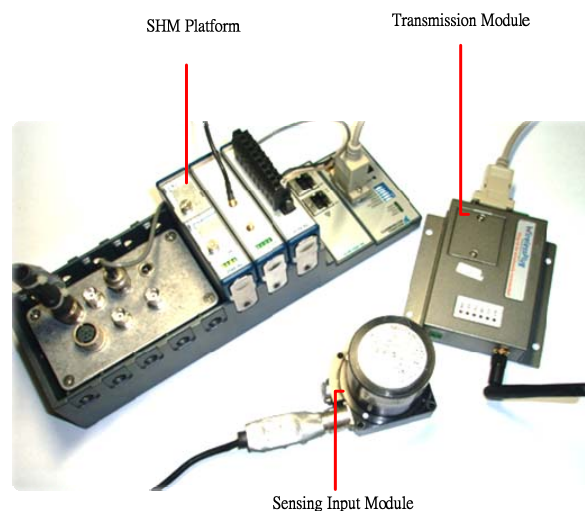


Figure 10: The SHM Prototype

The details of the customized sliver module are shown in Figure 11. A total of seven connectors are mounted in the box. Both the velocity meter and the accelerometer can be connected to the two sensor connectors located in the rightmost column for different applications. For the micro-vibration mode, two measurement resolutions can be selected by using the built-in 10 V / Kine or 1 V / Kine converters. Up to 16 sensors can be powered simultaneously by the customized unit. In addition, two optional modules, a GPS module, and a memory card module for depositing the collected raw data can be installed adjacent to the input module. These two modules enable an easy extension of the functionality and mobility of the platform.

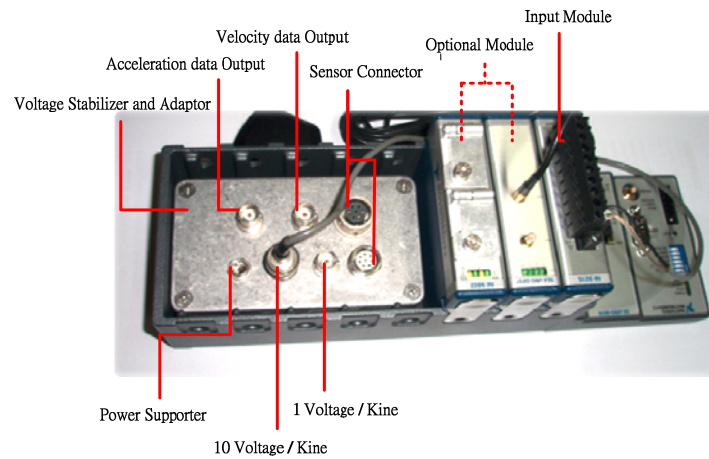


Figure 11: the SHM Monitoring Platform

In order to correctly execute the proposed algorithm in the prototype, the SHM algorithm is incorporated in the firmware of the mobile module. The corresponding software can be divided into two parts: the onsite program in the SHM platform and the demonstration program in the remote server where all the structure damage information is collected and displayed. As shown in Figure 12, the on-site program is subdivided into four parts: Data Pre-Processing, Coefficient Extraction, Health Condition Diagnosis, and GPRS & Wireless Module.

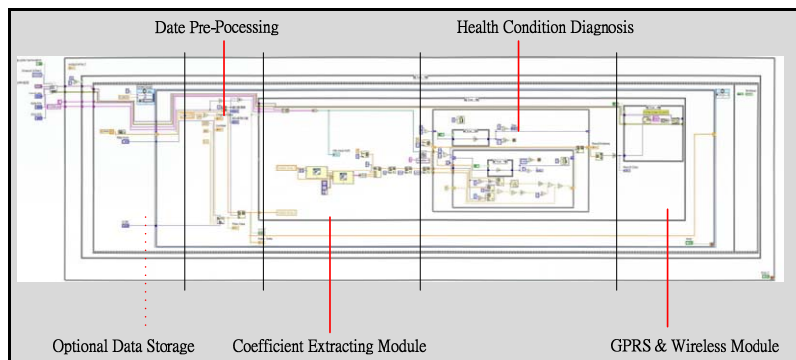


Figure 12: the On-Site Program

4.1 DATA PRE-PROCESSING

The Pre-Processing program performs three main functions: input data collection, digital filter design, and data size adjustment/setting for SHM processing. The use of the Pre-Processing program helps to eliminate the undesired noise successfully from the ambient environment to ensure clarity in the input data. In this study, the data sample rate was selected as 200 Hz, and a band-pass filter was chosen to filter out the unwanted high and low frequency sets of 90 Hz and 0.1 Hz. This also helped to eliminate errors arising from the voltage conversion between the analog and digital signals to enable accurate collection of desired data.

4.2 COEFFICIENT EXTRACTION MODULE

The Coefficient Extraction module was designed based on the two proposed SHM algorithms. In this study, the ARX and AR-ARX models are first established and then implemented with the desired order of settings. The Coefficient Extraction module assists in transforming the time history of the structural responses into array form quickly, and the damage condition of the structure can subsequently be evaluated in the next stage by making a comparison between the damage data and the collected database.

4.3 HEALTH CONDITION DIAGNOSIS

The condition and location of the structural damage are determined by the embedded NB-based SHM algorithm. By making a comparison between the arrays calculated from the previous block and the stored database, the probability of occurrence of all damage conditions for either earthquake excitation or micro-vibration modes is estimated by a designated loop, which subsequently enables the detection of the location and condition of the structural damage.

4.4 GPRS & WIRELESS MODULE

In order to achieve the goal of real-time monitoring following the analysis and classification of the damage, the GPRS Module is used to transfer the data back to the monitoring server. To ensure the security of the data being transmitted, it is encrypted. In this study, a technique to safely encrypt and decrypt the data by adding an initial AA string at the beginning of data transmission chain was developed. Only data with are equipped with this characteristic will then be received.

The mobile SHM prototype can be applied to real life structures by combining the software and hardware described above. The mobile SHM prototype has been designed to classify the structural damage condition within a span of one minute.

5 PRACTICAL VERIFICATION

The performance of the SHM prototype was tested using experimental verification. The eight-storey downscaled benchmark mounted on the shaking table at NCREE was used as the practical test structure. Structural damage testing was simulated by loosening four bolts on the third floor which represented damage condition 4. The response under both ambient and earthquake vibration modes was measured using the top three sensors (6F, 7F, and 8F) deployed on the structure.

By comparing the AR-ARX and ARX array obtained from the vibration data with the database deposited in the on-site SHM prototype, the structural health condition can be immediately evaluated. In addition, to demonstrate the feasibility of remote monitoring, the server was chosen at the headquarters of the National Science Council (NSC), and the health condition of the structure was immediately transmitted by the GPRS service, since the proposed SHM system only requires a small bandwidth. The locations of the benchmark and the monitoring server are shown in Figure 13.

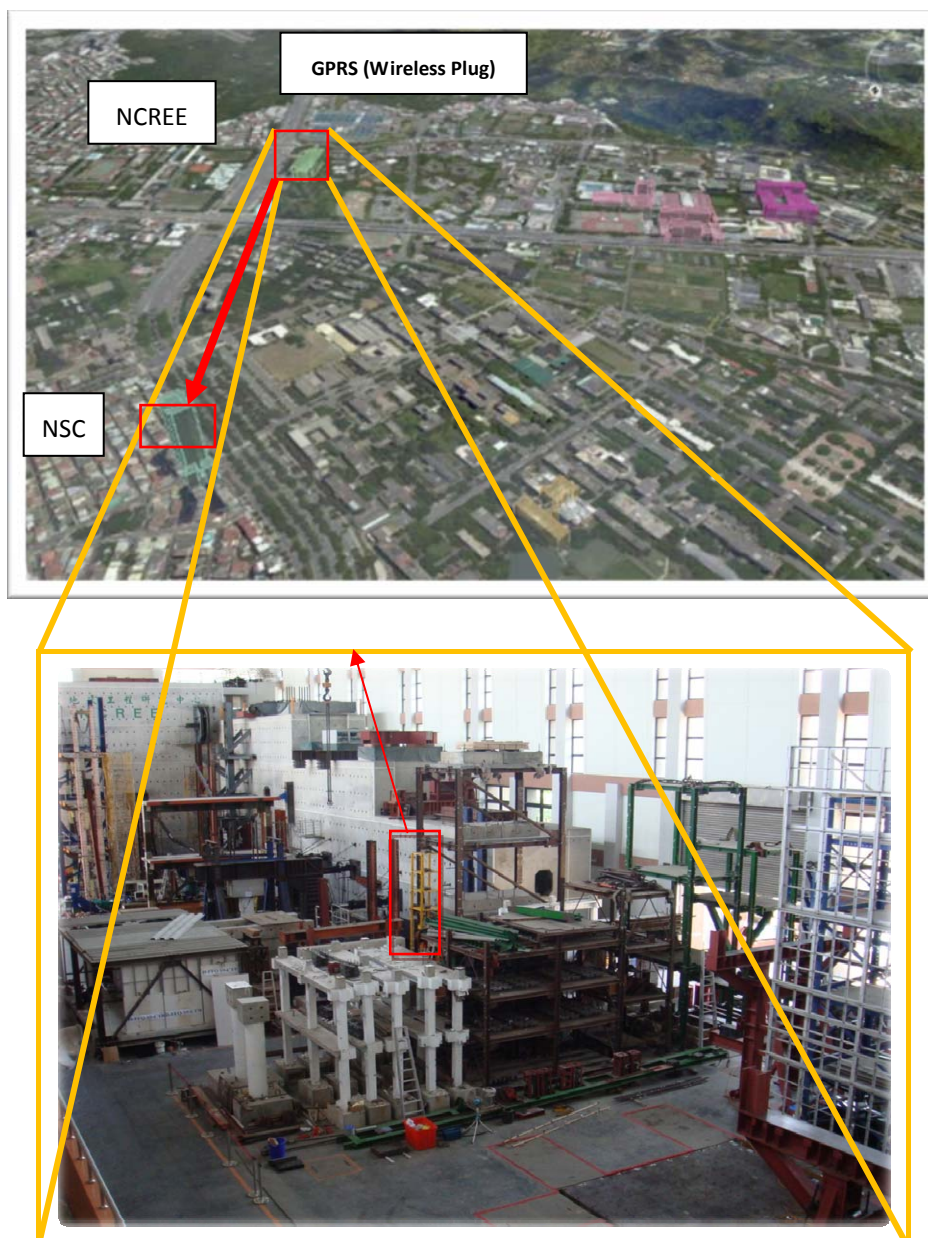


Figure 13: Location of the benchmark and the monitoring server

The result from real-time monitoring is shown in Figure 14. It shows that SHM results can be determined by either the earthquake mode or the micro-vibration mode. The switching criterion between these two modes is set to enable an acceleration of 5 gal. If the largest measured acceleration is less than 5 gal, the structural response is measured and processed every 20 seconds, and the results are displayed sequentially in the top left-hand portion of the figure. The numbers shown in the panel represent

the classification result. As mentioned in the previous section, to avoid false alarms in practical applications, the SHM algorithm operates three times a minute with the two-layer union concept to determine the condition and location of the structure damage as depicted in Figure 14. The damage level of the structure is either none, slight, moderate, severe, extreme, or ultimate, and is shown in the middle of the figure. The detected damage location is highlighted on the structure. In addition, the SHM system was also tested by shaking the benchmark structure under earthquakes. The earthquake mode was launched once the detected acceleration value became greater than 5 gal. The union result from the three different sensors is shown in the bottom-left hand corner of Figure 14. The experiment result clearly demonstrated that both the damage condition, which was slight, and the location, i.e. the third floor, could be detected with precision by the two-mode SHM system.

In addition, not only can real-time structural damage be monitored by the mobile SHM prototype, the embedded parameters can also be remotely controlled. This flexible monitoring design can make the SHM system an optimal system for facilitating varied conditions and permit the immediate evaluation of any structural damage. Characteristics like high mobility and prompts on-site processing of the proposed mobile SHM system have finally been implemented.

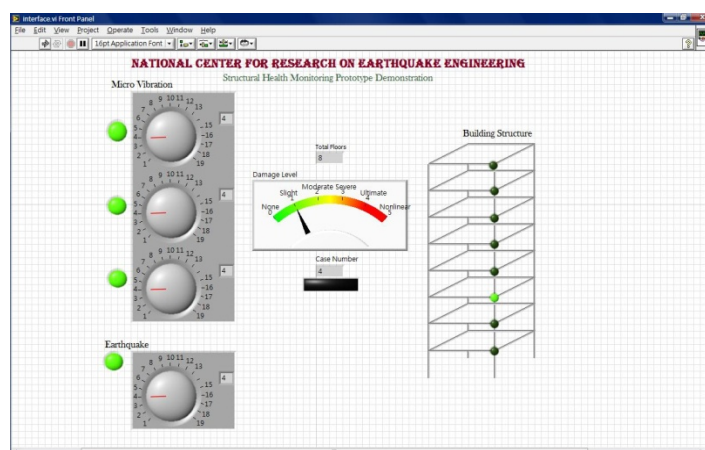


Figure 14: the Real-Time Monitoring Interface

6 SUMMARY AND CONCLUSION

A bio-inspired two-mode structural health monitoring (SHM) system based on the Naïve Bayes (NB) classification method was presented in this paper. Since research focus on the bio-inspired concept for engineering has only recently evolved, a novel SHM algorithm utilizing the array expression data of the Deoxyribonucleic acid (DNA) of the structures was developed. Based on the vibration mode, the proposed SHM algorithm can switch between a two-tier AR-ARX process for micro-vibration and an ARX process for earthquake excitation. The health condition of the structure is then determined by classifying the obtained array expression data using the NB method. Moreover, the union concept in probability was introduced to improve the accuracy of the system.

To verify the performance and reliability of the SHM algorithm, a downscaled eight-storey steel building located at the shaking table of NCREE was used as the

benchmark structure. The structural damage was simulated by loosening four of the 16 bolts in each floor (1/4 of the beam-column connection). The structural response was then determined for different damage levels and locations for inclusion in the structural health monitoring database. Experimental results have demonstrated that the approximate condition and location of the damage can be quickly determined immediately after the occurrence of an earthquake. A more precise result can be achieved in the micro-vibration detection mode.

To implement the proposed SHM system in a practical application, a SHM prototype consisting of three individual modules namely, the input sensing module, the transmission module, and the SHM platform was developed. The employed sensor first measures the structural response, and subsequently, the SHM mode corresponding to the excitation is chosen automatically by the system to rapidly evaluate the health condition of the structure using a preset criterion. Test results from the ambient vibration and shaking table test have shown that the condition and location of the benchmark structure damage can be successfully monitored by the SHM prototype system and can be instantly transmitted to a remote server to facilitate real-time monitoring.

Implementing the bio-inspired two-mode SHM practically has been demonstrated in this paper. The bio-inspired concept is made possible by the successful integration of software and hardware. With its unique mobility and powerful processing capacity, it is expected that the proposed SHM system can be applied to SHM networks in practical applications in the near future.

REFERENCES

- [1] Hickman, G.A.; Gerardi, J.J.; Feng, Y., 1991. Application of smart structures to aircraft health monitoring, *Journal of Intelligent Material Systems and Structures*, v 2, n 3, p 411-430.
- [2] Aktan, A.E.; Helmicki, A.J.; Hunt, V.J., 1998. Issues in health monitoring for intelligent infrastructure, *Smart Materials and Structures*, v 7, n 5, p 674-92.
- [3] Pines, D.J.; Lovell, P.A., 1998. Conceptual framework of a remote wireless health monitoring system for large civil structures, *Smart Materials and Structures*, v 7, n 5, p 627-36.
- [4] Tanner, N.A.; Wait, J.R.; Farrar, C.R.; Hoon Sohn, 2003. Structural health monitoring using modular wireless sensors, *Journal of Intelligent Material Systems and Structures*, v 14, n 1, p 43-56.
- [5] Wang, Yang; Lynch, Jerome P.; Law, Kincho H., 2007. A wireless structural health monitoring system with multithreaded sensing devices: Design and validation, *Structure and Infrastructure Engineering*, v 3, n 2, p 103-120.
- [6] Lynch, Jerome Peter; Law, Kincho H.; Kiremidjian, Anne S.; Carryer, Ed.; Farrar, Charles R.; Sohn, Hoon; Allen, David W.; Nadler, Brett; Wait, Jeannette R., 2004. Design and performance validation of a wireless sensing unit for structural monitoring applications, *Structural Engineering and Mechanics*, v 17, n 3-4, p 393-408.

- [7] Buckner, B.D.; Markov, V.; Li-Chung Lai; Earthman, J.C., 2008. Laser-scanning structural health monitoring with wireless sensor motes, *Optical Engineering*, v 47, n 5, p 1-9.
- [8] Zimmerman, Andrew T.; Shiraishi, Michihito; Swartz, R. Andrew; Lynch, Jerome P., 2008. Automated modal parameter estimation by parallel processing within wireless monitoring systems, *Journal of Infrastructure Systems*, v 14, n 1, p 102-113.
- [9] Mascarenas, David D.L.; Flynn, Eric B.; Todd, Michael D.; Overly, Timothy G.; Farinholt, Kevin M.; Park, Gyuhae; Farrar, Charles R., 2010. Development of capacitance-based and impedance-based wireless sensors and sensor nodes for structural health monitoring applications, *Journal of Sound and Vibration*, v 329, n 12, p 2410-2420.
- [10] Boller, C., 2000. Next generation structural health monitoring and its integration into aircraft design, *International Journal of Systems Science*, v 31, n 11, p 1333-49.
- [11] Hu, N.; Wang, X.; Fukunaga, H.; Yao, Z.H.; Zhang, H.X.; Wu, Z.S., 2001. Damage assessment of structures using modal test data, *International Journal of Solids and Structures*, v 38, n 18, p 3111-3126.
- [12] Johnson, T.J.; Brown, R.L.; Adams, D.E.; Schiefer, M., 2004. Distributed structural health monitoring with a smart sensor array, *Mechanical Systems and Signal Processing*, v 18, n 3, p 555-72.
- [13] Hera, Adriana; Hou, Zhikun, 2004. Application of wavelet approach for ASCE structural health monitoring benchmark studies, *Journal of Engineering Mechanics*, v 130, n 1, p 96-104.
- [14] Udawadia, Firdaus E.; Proskurowski, Wlodek, 1998. A memory-matrix-based identification methodology for structural and mechanical systems, *Earthquake Engineering and Structural Dynamics*, v 27, n 12, p 1465-1481.
- [15] Zhang, Jian; Sato, Tadanobu; Iai, Susumu, 2006. Support vector regression for on-line health monitoring of large-scale structures, *Structural Safety*, v 28, n 4, p 392-406, September
- [16] Carden, E.P.; Brownjohn, J.M.W., 2008. ARMA modelled time-series classification for structural health monitoring of civil infrastructure, *Mechanical Systems and Signal Processing*, v 22, n 2, p 295-314.
- [17] Sohn, Hoon; Czarnecki, Jerry A.; Farrar, Charles R., 2000. Structural health monitoring using statistical process control, *Journal of structural engineering* New York, N.Y., v 126, n 11, p 1356-1363.
- [18] Sohn, Hoon; Farrar, C.R., 2001. Damage diagnosis using time series analysis of vibration signals, *Smart Materials and Structures*, v 10, n 3, p 446-51.
- [19] L. Ljung, "System Identification: Theory for the User", Prent-Hall, Inc. Upper Saddle River, NJ, USA, 1986.
- [20] T.R. Golub, D.K. Slonim, P. Tamayo, C. Huard, M. Gaasenbeek, J.P. Mesirov, H. Coller, M.L. Loh, J.R. Downing, M.A. Caligiuri, C.D. Bloomfield and E.S. Lander, "Molecular Classification of Cancer: Class Discovery and Class

Prediction by Gene Expression Monitoring”, *Science* 15, Vol. 286. no. 5439, pp. 531-537, 10.1126/science.286.5439.531, October 1999.

- [21] Donna K. Slonim, Pablo Tamayo, Jill P. Mesirov, Todd R. Golub and Eric S. Lander, “Class Prediction and Discovery Using Gene Expression Data”, Annual Conference on Research in Computational Molecular Biology, Proceedings of the 4th annual international conference on Computational molecular biology, pp. 263-272, 1-58113-186-0, Tokyo, Japan, 2000.